

Quantum-based Feature Selection for Multi-Classification Problem in Complex Systems with Edge Computing

Wenjie Liu¹, Junxiu Chen², Yuxiang Wang³, Peipei Gao⁴, Zhibin Lei⁵, and Xu Ma⁶

Jiangsu Engineering Center of Network Monitoring, Nanjing University of Information Science and Technology, Nanjing 210044, P.R.China¹

School of Computer and Software, Nanjing University of Information Science and Technology, Nanjing 210044, P.R.China²

Jiangsu Engineering Center of Network Monitoring, Nanjing University of Information Science and Technology, Nanjing 210044, P.R.China³

Jiangsu Engineering Center of Network Monitoring, Nanjing University of Information Science and Technology, Nanjing 210044, P.R.China⁴

Hong Kong Applied Science and Technology Research Institute(ASTRI),Hong Kong 999077, China⁵

School of Software, Qufu Normal University,Shandong 273165, China⁶

Abstract. The complex systems with edge computing require a huge amount of multi-feature data to extract appropriate insights for their decision-making, so it is important to find a feasible feature selection method to improve the computational efficiency and save the resource consumption. In this paper, a quantum-based feature selection algorithm for the multi-classification problem, namely QReliefF, is proposed, which can effectively reduce the complexity of algorithm and improve its computational efficiency. First, all features of each sample are encoded into a quantum state by performing operations CMP and R_y , then the amplitude estimation is applied to calculate the similarity between any two quantum states (i.e., two samples). According to the similarities, the Grover-Long method is utilized to find the nearest k neighbor samples, and then the weight vector is updated. After a certain number of iterations through the above process, the desired features can be selected with regards to the final weight vector and the threshold τ . Compared with the classical ReliefF algorithm, our algorithm reduces the complexity of similarity calculation from $O(MN)$ to $O(M)$, the complexity of finding the nearest neighbor from $O(M)$ to $O(\sqrt{M})$, and resource consumption from $O(MN)$ to $O(M\log N)$. Meanwhile, compared with the quantum Relief algorithm, our algorithm is superior in finding the nearest neighbor, reducing the complexity from $O(M)$ to $O(\sqrt{M})$. Finally, in order to verify the feasibility of our algorithm, a simulation experiment based on Rigetti with a simple example is performed.

Keywords: Quantum ReliefF algorithm, Edge computing, Complex systems, Feature selection, Amplitude estimation, Grover-Long method, Rigetti

1 Introduction

Complex systems [1] are nonlinear systems composed of agents that can act with local environmental information, which require big data to extract appropriate insights for their decision-making. In the cloud computing [2] [3] [4] [5], the data transmission delay between the data sources and the cloud centers is problematic for many complex systems where responses are usually required to be time critical or real-time. Instead, a recently emerging computation paradigm, edge computing [6] [7] [8] [9], is promising to cater for these requirements, as edge computing resources are deployed data sources which support time critical or real-time data processing and analysis. As we all know, the computing resources and storage resources of most intelligent terminals are very limited, which places higher requirements on the computing performance of algorithms, especially machine learning algorithms, in complex systems with edge computing.

Machine learning [10] [11] continuously improves its performance through “experience”, where experience generally originates from massive data. At present, many machine learning algorithms based on massive data [12] [13] [14] have been proposed. In the practical scenario, the amount of data available for training is getting larger and larger, while the characteristics of data are becoming more and more abundant. Those data with redundant or unrelated features will cause the problem of “curse of dimensionality” [15], which greatly increases the computational complexity of the algorithm. One of the possible solutions is the dimension reduction [16], and the other is the feature selection [17].

Relief algorithm [18] is a well-known feature selection algorithm for the two-classification problem. It is widely used because of its excellent classification effect. However, the limitation of this algorithm is that it can only perform the binary classification, and the efficiency of the algorithm will be greatly affected when the data size and feature size increase. To extend the application of the algorithm, Kononenko [19] proposed a new feature selection algorithm for the multi-classification problem, namely Relief algorithm. It has the advantages of simple principle, convenient implementation and good results, and has been widely applied in various fields [20] [21] [22].

On the other hand, since Benioff [23] and Feynman [24] explored the theoretical possibilities of quantum computing, some excellent results have been proposed one after another. For instance, Shor’s algorithm [25] solves the problem of integer factorization in polynomial time. Grover’s algorithm [26] has a quadratic speedup to the problem of conducting a search through some unstructured database. These excellent results have prompted people to think about how to apply this computing power into machine learning algorithms. And thus a new research hotspot, quantum machine learning [27] [28] [29] [30] [31] [32], has gradually formed. Although quantum technology provides a certain improvement in storage and computing power, the “curse of dimensionality” problem still exists in quantum machine learning. Therefore, the quantum-based dimensionality reduction method still has important research value. In 2018, Liu et al. [33] proposed a quantum Relief algorithm (namely QRelief algorithm) for the

two-classification problem, which reduces the complexity of similarity calculation from $O(MN)$ to $O(M)$.

As we know, in the application scenario of edge computing, there are various multi-classification problems based on distributed, massive and large-feature data. The objective of this study is to design a feasible feature selection method which can effectively get rid of redundant or unrelated features in machine learning, reducing the computation load of intelligent terminals, and thus meet the requirement of real-time data processing and analysis in edge computing. In this paper, we introduce some quantum technologies (such as *CMP* operation, amplitude estimation and Grover-Long method), and propose a quantum-based feature selection algorithm, namely QReliefF algorithm, for the multi-classification problem.

The main contributions of our work are:

(1) A quantum method is proposed to solve the problem of feature selection for the multi-classification problem in complex systems with edge computing. The proposed method fully demonstrates the quantum parallel processing capabilities that classical computing cannot match, and significantly reduces the computational complexity of the algorithm.

(2) The problem of finding nearest neighbor samples is firstly transformed into the similarity calculation of two quantum states (i.e., calculating their inner product) in quantum computing, and the Grover-long method is utilized to speed up the search of the targets.

(3) A simulation experiment based on Rigetti is performed to verify the feasibility of our algorithm.

The outline of this paper is as follows: The classic ReliefF algorithm is briefly reviewed in Sect. 2, and the proposed quantum ReliefF algorithm is proposed in detail in Sect. 3. Then, we illustrate the process of the algorithm with a simple example in Sect. 4, and perform the simulation experiment on Rigetti in Sect. 5. Subsequently, the efficiency of the algorithm is analyzed in Sect. 6, and the brief conclusion and discussion are summarized in the last section.

2 Review of ReliefF algorithm

ReliefF algorithm [19] is a feature selection algorithm which is used to handle the multi-classification problem. Before introducing our proposed quantum algorithm, let us review the detailed process of the algorithm.

Without loss of generality, suppose there are M samples with N features, and they can be divided into P classes:

$$C_p = \{v_q \mid v_q \in \mathbb{R}^N, q = 1, 2, \dots, M_p\}, p \in \{1, 2, \dots, P\}, \quad (1)$$

where v_q is the q -th N -feature sample that belongs to Class C_p , $v_q = (v_{q1}, v_{q2}, \dots, v_{qN})^T$. And the weight vector of N features $WT = (wt_1, wt_2, \dots, wt_N)^T$ is initialized to all zeros, the upper limit of iteration is T , and the relevance threshold (that differentiate the relevant and irrelevant features) is τ ($0 \leq \tau \leq 1$). The main steps of ReliefF algorithm are as follows (its pseudo code can be seen in Algorithm 1).

Algorithm 1: ReliefF algorithm

```

1 Init  $WT = (0, \dots, 0)^T$ 
2 for  $t = 1$  to  $T$  do
3   Pick a sample  $u$  randomly
4   Find  $k$  nearest neighbor samples  $H_j$  from the same class of sample  $u$ .
5   for  $C_p \neq \text{class}(u)$  do
6     Find  $k$  nearest neighbor samples  $M_j(C_p)$  from the different Class  $C_p$ 
7   end
8   for  $i = 1$  to  $N$  do
9      $WT[i] = WT[i] - \sum_{j=1}^k \text{diff}(i, u, H_j) +$ 
        $\sum_{C_p \notin \text{class}(u)} \left[ \frac{p(C_p)}{1-p(\text{class}(u))} \sum_{j=1}^k \text{diff}(i, u, M_j(C_p)) \right]$ 
10  end
11 end
12 Select the most relevant features according to  $WT$  and  $\tau$ 

```

At each iteration, ReliefF randomly selects a sample u , and then searches for k nearest neighbor samples by cosine distance from each class. The closest same-class sample is called H_j , and the closest different-class sample is called $M_j(C_p)$, where $j = \{1, 2, \dots, k\}$. The updating weight vector formula is shown as follows,

$$\begin{aligned}
 WT[i] &= WT[i] - \sum_{j=1}^k \text{diff}(i, u, H_j) \\
 &+ \sum_{C_p \notin \text{class}(u)} \left[\frac{p(C_p)}{1-p(\text{class}(u))} \sum_{j=1}^k \text{diff}(i, u, M_j(C_p)) \right]
 \end{aligned} \tag{2}$$

where $p(C_p)$ represents the probability of randomly extracting samples of Class C_p , and the definition of $\text{diff}(i, u, v)$ function is as follows,

$$\text{diff}(i, u, v) = \begin{cases} \frac{|u[i]-v[i]|}{\max(i)-\min(i)} & i \text{ is continuous} \\ 0 & u_i = v_i \\ 1 & u_i \neq v_i \end{cases} . \tag{3}$$

After iterating T times, the final weight vector is obtained. Through the relevance threshold τ , we can retain relevant features and discard irrelevant features.

ReliefF algorithm is an extension of Relief algorithm that extends the two-classification problem to multi-classification scenario. However, with the increase of category size, sample size and sample features, ReliefF algorithm will also face with the problem of “dimension disaster”, and the speed of the algorithm will also drop sharply. So, how to improve the efficiency of ReliefF algorithm becomes an urgent problem to be solved.

3 The proposed QRelieFF algorithm

In order to implement the feature selection for the multi-classification problem in complex systems with edge computing, a feasible quantum ReliefF algorithm is introduced in this section. Suppose the sample sets $C_p = \{v_q = (v_{q1}, v_{q2}, \dots, v_{qN})^T \mid v_q \in \mathbb{R}^N, q = 1, 2, \dots, M_p\}$ (p represents the category of classification, $p \in \{1, 2, \dots, P\}$), the weight vector WT , the upper limit T , and the relevance threshold τ are the same as classical ReliefF algorithm defined in Sect. II. Different from the classical one, all the features of each sample are represented as a quantum superposition state, thus the problem of finding nearest neighbor samples is transformed into the similarity calculation of two quantum states (i.e., calculating their inner product). And the similarity between any two samples can be calculated in parallel in the way of quantum mechanics. Algorithm 2 describes the process of our algorithm in detail, and the specific steps are as bellow.

3.1 State preparation

In order to store classical information in quantum states, we need to normalize the sample sets:

$$C_p \rightarrow \bar{C}_p = \{\bar{v}_q = (\bar{v}_{q1}, \bar{v}_{q2}, \dots, \bar{v}_{qN})^T\}, \quad (4)$$

where

$$\bar{v}_{qi} = \frac{v_{qi}}{\sqrt{\sum_{i=1}^N |v_{qi}|^2}}, i = 1, 2, \dots, N. \quad (5)$$

Obviously, \bar{v}_{qi} is a real number, and $\bar{v}_{qi} \in (0, 1)$. Then we prepare the initial quantum states as below,

$$|\phi_p\rangle_q = \frac{1}{\sqrt{N}} |q\rangle \sum_{i=0}^{N-1} |i\rangle |1\rangle \left(\sqrt{1 - |\bar{v}_{qi}|^2} |0\rangle + \bar{v}_{qi} |1\rangle \right), \quad (6)$$

where $|\phi_p\rangle_q$ corresponds to the quantum state of the q -th sample that belongs to Class \bar{C}_p , and \bar{v}_{qi} represents the i -th eigenvalue of the q -th sample. Assume our initial state is $|q\rangle |0\rangle^{\otimes n} |1\rangle |0\rangle$ ($n = \lceil \log_2(N) \rceil$), the construction scheme of the quantum state $|\phi_p\rangle_q$ includes the following steps.

First, we perform Hadamard and *CMP* operations for $|0\rangle^{\otimes n}$ and get a new state:

$$|0\rangle^{\otimes n} \xrightarrow{\text{H and CMP operations}} \frac{1}{\sqrt{N}} \sum_{i=0}^{N-1} |i\rangle, \quad (7)$$

and its circuit diagram is shown in Fig. 1, where the definition of *CMP* operation is

$$\text{CMP } |i\rangle |N\rangle |0\rangle = \begin{cases} |i\rangle |N\rangle |0\rangle, & i < N \\ |i\rangle |N\rangle |1\rangle, & i \geq N \end{cases} \quad (8)$$

Algorithm 2: Quantum ReliefF algorithm

1 *Init* $WT = (0, \dots, 0)^T$
2 *Normalized the sample sets:* $C_p \rightarrow \bar{C}_p$
3 *prepare quantum states for all samples by operations CMP and R_y ,*
respectively. $|\phi_p\rangle_q = \frac{1}{\sqrt{N}} |q\rangle \sum_{i=0}^{N-1} |i\rangle |1\rangle \left(\sqrt{1 - |\bar{v}_{qi}|^2} |0\rangle + \bar{v}_{qi} |1\rangle \right)$
4 **for** $t = 1$ **to** T **do**
5 *Select a state* $|\phi\rangle$ *from* $\{|\phi_p\rangle_q\}$ *randomly which corresponds to* u
6 *Perform swap operation on* $|\phi\rangle$ *and obtain*
 $|\varphi\rangle = \frac{1}{\sqrt{N}} |l\rangle \sum_{i=0}^{N-1} |i\rangle \left(\sqrt{1 - |\bar{u}_i|^2} |0\rangle + \bar{u}_i |1\rangle \right) |1\rangle$
7 *The similarity information coded into quantum state*
 $|\beta\rangle_p = \frac{1}{\sqrt{M_p}} \sum_{q=1}^{M_p} |q\rangle |\bar{v}_q - \bar{u}\rangle$ *through swap test, the inner product and*
amplitude estimation operations
8 *The nearest k samples in each class are obtained by Grover-Long method*
9 **for** $i = 1$ **to** N **do**
10 $WT[i] = WT[i] - \sum_{j=1}^k \text{diff}(i, \bar{u}, H_j) +$
 $\sum_{\bar{C}_p \notin \text{class}(\bar{u})} \left[\frac{p(\bar{C}_p)}{1 - p(\text{class}(\bar{u}))} \sum_{j=1}^k \text{diff}(i, \bar{u}, M_j(\bar{C}_p)) \right]$
11 **end**
12 **end**
13 $\overline{WT} = (1/T) WT$
14 **for** $i = 1$ **to** N **do**
15 **if** $(\overline{WT}_i \geq \tau)$ **then**
16 *The i -th feature is relevant;*
17 **else**
18 *The i -th feature is not relevant;*
19 **end**
20 **end**

The function of *CMP* operation is to cut the quantum state larger than N , and its circuit diagram is shown in Fig. 2. $|i\rangle$ and $|N\rangle$ represent a single qubit. The implementation of *CMP* operation needs to repeatedly implement such a circuit n times. After measurement, if the lowest register is $|1\rangle$, it means that $i > N$.

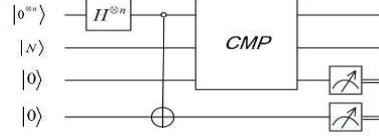


Fig. 1: Quantum circuit of getting $\frac{1}{\sqrt{N}} \sum_{i=0}^{N-1} |i\rangle$, and H is the Hadamard operation, \circ represents the control qubit conditional being set to zero.

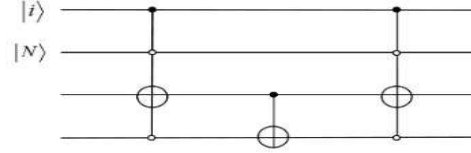


Fig. 2: Quantum circuit of *CMP* operation, and \bullet represents the control qubit conditional being set to one.

Next, we perform the unitary rotation operation R_y :

$$R_y(2\sin^{-1}\bar{v}_{qi}) = \begin{bmatrix} \sqrt{1 - |\bar{v}_{qi}|^2} & -\bar{v}_{qi} \\ \bar{v}_{qi} & \sqrt{1 - |\bar{v}_{qi}|^2} \end{bmatrix}, \quad (9)$$

on the last qubit to obtain our target quantum state $|\phi_p\rangle_q$,

$$\frac{1}{\sqrt{N}} |q\rangle \sum_{i=0}^{N-1} |i\rangle |1\rangle \left(\sqrt{1 - |\bar{v}_{qi}|^2} |0\rangle + \bar{v}_{qi} |1\rangle \right). \quad (10)$$

3.2 Similarity calculation

After the state preparation, the information of the samples is encoded into the quantum superposition state $\{|\phi_p\rangle_q\}$. In this paper, we use the cosine distance

to define the similarity between the random sample \bar{u} and other sample (e.g., \bar{v}_q),

$$s(\bar{u}, \bar{v}_q) \doteq |\cos \theta|^2 = \frac{|\langle \bar{u} | \bar{v}_q \rangle|^2}{|\bar{u}|^2 \cdot |\bar{v}_q|^2}. \quad (11)$$

Referring to Eqs. (4) and (5), $|\bar{u}|^2$ and $|\bar{v}_q|^2$ are 1, Eq. 11 can be simplified as follows,

$$s(\bar{u}, \bar{v}_q) = |\langle \bar{u} | \bar{v}_q \rangle|^2. \quad (12)$$

First, $|\phi\rangle$ (i.e., the sample \bar{u}) is randomly selected from $\{|\phi_p\rangle_q\}$ which is the l -th sample in Class \bar{C}_p , as shown in the following equation,

$$|\phi\rangle = \frac{1}{\sqrt{N}} |l\rangle \sum_{i=0}^{N-1} |i\rangle |1\rangle \left(\sqrt{1 - |\bar{u}_i|^2} |0\rangle + \bar{u}_i |1\rangle \right). \quad (13)$$

Then, a *swap* operation is performed on $|\phi\rangle$ to get

$$|\varphi\rangle = \frac{1}{\sqrt{N}} |l\rangle \sum_{i=0}^{N-1} |i\rangle \left(\sqrt{1 - |\bar{u}_i|^2} |0\rangle + \bar{u}_i |1\rangle \right) |1\rangle. \quad (14)$$

Next, a *swap test* (its circuit is given in Fig.3) is performed on $(|\varphi\rangle, |\phi_p\rangle_q)$ and obtain

$$|\psi\rangle = \frac{1}{2} |0\rangle (|\varphi\rangle |\phi_p\rangle_q + |\phi_p\rangle_q |\varphi\rangle) + \frac{1}{2} |1\rangle (|\varphi\rangle |\phi_p\rangle_q - |\phi_p\rangle_q |\varphi\rangle). \quad (15)$$

Fig. 3: Quantum circuit of *swap test* operation, and the symbol of two crosses connected by a line represents the *swap* operation.

From Eq. (15), we know the probability of measurement result being $|1\rangle$ is

$$\begin{aligned} P_q^l(1) &= \langle \psi | |1\rangle \langle 1| \otimes I \otimes I | \psi \rangle \\ &= \left[\frac{1}{2} \langle 1 | \left(\langle \varphi | \langle \phi_p |_q - \langle \phi_p |_q \langle \varphi | \right) \right] |1\rangle \langle 1| \otimes I \otimes I \right. \\ &\quad \left. \left[\frac{1}{2} \langle 1 | \left(|\varphi\rangle |\phi_p\rangle_q - |\phi_p\rangle_q |\varphi\rangle \right) \right] \right] \\ &= \frac{1}{2} - \frac{1}{2} \left| \langle \varphi | \phi_p \rangle_q \right|^2, \end{aligned} \quad (16)$$

In addition, the inner product between $|\varphi\rangle$ and $|\phi_p\rangle_q$ (i.e., the prepared state) can be calculated as below,

$$\langle \varphi | \phi_p \rangle_q = \frac{1}{N} \sum_i (\bar{u}_i) * \bar{v}_{qi} = \frac{1}{N} \langle \bar{u} | \bar{v}_q \rangle. \quad (17)$$

Combining Eq. (16) with Eq. (17), we can get the similarity between samples \bar{u} and \bar{v}_q ,

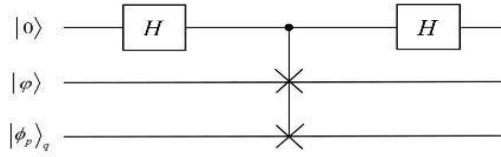
$$s(\bar{u}, \bar{v}_q) = \left(1 - 2P_q^{l(\bar{C}_p)}(1)\right) N^2 \quad (18)$$

Since N is a constant value and $\langle \bar{u} | \bar{v}_q \rangle$ is the angle cosine between the random sample \bar{u} and other sample \bar{v}_q (e.g., in Class \bar{C}_p), then the smaller $s(\bar{u}, \bar{v}_q)$ is, the smaller cosine distance is, which indicates that these two samples are more similar.

Then we can rewrite Eq. (15) as bellow:

$$|\alpha\rangle_p = \frac{1}{\sqrt{M_p}} \sum_{q=1}^{M_p} |q\rangle \left(\sqrt{1 - s(\bar{u}, \bar{v}_q)} |0\rangle + \sqrt{s(\bar{u}, \bar{v}_q)} |1\rangle \right). \quad (19)$$

3.3 Finding the nearest neighbor samples



First, the quantum amplitude estimation method [34] is applied to store the similarity of the sample \bar{u} and \bar{v}_q in the last qubit,

$$|\beta\rangle_p = \frac{1}{\sqrt{M_p}} \sum_{q=1}^{M_p} |q\rangle |s(\bar{u}, \bar{v}_q)\rangle, \quad (20)$$

where $p \in \{1, 2, \dots, P\}$, and its quantum circuit diagram is given in Fig. 4.

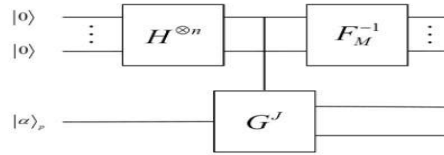


Fig. 4: Quantum circuit of amplitude estimation operation, G^J represents J iterations of Grover-Long method [35] and F_M^{-1} represents the inverse Fourier transform [36].

In the Grover-Long method [35], one iteration can be divided into four operations, i.e., $G = -WI_0W^{-1}O$, and its quantum circuit is shown in Fig. 5. O

is an oracle operation which performs a phase inversion on the targets:

$$O = e^{i\phi} |v\rangle \langle v| + \sum_{\tau=0, \tau \neq v}^{2^n-1} |\tau\rangle \langle \tau|, \quad (21)$$

where v is the position of $e^{i\phi}$ in the diagonal matrix. The position v of $e^{i\phi}$ is divided into two cases. If v is odd, the $u_1(\phi)$ operation will be applied to the lowest qubit,

$$u_1(\phi) = \text{diag} [1, e^{i\phi}]. \quad (22)$$

If v is even, $X, u_1(\phi), X$ operations will be applied to the lowest qubit.

Besides, I_0 is a conditional phase shift operation which performs a phase inversion on $|0\rangle$:

$$I_0 = e^{i\phi} |0\rangle \langle 0| + \sum_{\tau=1}^{2^n-1} |\tau\rangle \langle \tau| = \text{diag} [e^{i\phi}, 1, \dots, 1]_{2^n}, \quad (23)$$

$$\phi = 2 \arcsin \left(\frac{\sin \frac{\pi}{4J+2}}{\sin \eta} \right). \quad (24)$$

where $\sin \eta = \sqrt{\frac{M}{N}}$, J represents the number of iteration.

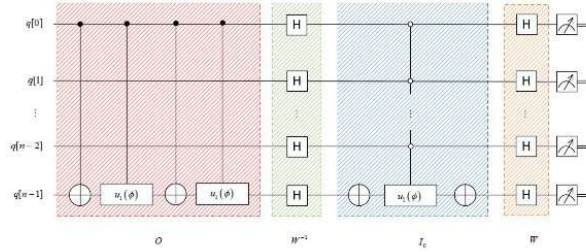


Fig. 5: Quantum circuit with one iteration in Grover-Long method [35], and $q[0]$ denotes the highest qubit, $q[n-1]$ denotes the lowest qubit.

Having obtained the state $|\beta\rangle_p$ (see Eq. (20)) through the amplitude estimation, we introduce a quantum minimum search algorithm [37] to find k nearest neighbor samples from Class \tilde{C}_p with the time complexity of $O(\sqrt{kM_p})$, and its quantum circuit is shown in Fig. 6.

Suppose the set $K = \{K_1, K_2, \dots, K_k\}$ represents the k nearest neighbor samples, so we should prepare $\lceil \sqrt{k} \rceil$ auxiliary qubits. As shown in Fig. 6, the operator W_s represents $W_s |\beta\rangle_p |0^{\otimes k}\rangle = |\beta\rangle_p |K_1\rangle |K_2\rangle \dots |K_k\rangle$, and $u_1(\phi)$ is the operator defined in Eq. (22). Let $d_0 = s(\bar{u}, \bar{v}_1)$, we can mark K_x when

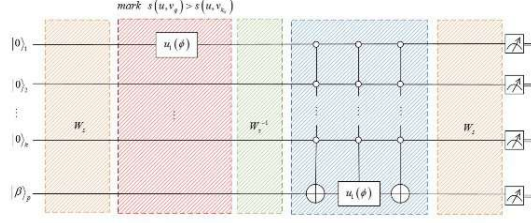


Fig. 6: Quantum circuit of finding k nearest neighbor samples.

$d_0 > s(\bar{u}, \bar{v}_{K_x}), x \in [1, k]$. Next, we can replace d_0 after one iteration, where d_0 is $\min\{s(\bar{u}, \bar{v}_{K_x})\}, x \in [1, k]$. We repeat the above steps several times until all samples in Class \bar{C}_p are compared. Finally, all index of k nearest neighbor samples in Class \bar{C}_p can be gotten according to the similarity.

3.4 Updating weight vector

After the above steps, we obtain the nearest neighbor samples (i.e., H_j and $M_j(\bar{C}_p)$) of the random sample \bar{u} . Then, we update the weight vector according to the updating weight vector formula as follows,

$$\begin{aligned}
 WT[i] &= WT[i] - \sum_{j=1}^k \text{diff}(i, \bar{u}, H_j) \\
 &+ \sum_{\bar{C}_p \notin \text{class}(\bar{u})} \left[\frac{p(\bar{C}_p)}{1 - p(\text{class}(\bar{u}))} \sum_{j=1}^k \text{diff}(i, \bar{u}, M_j(\bar{C}_p)) \right], \tag{25}
 \end{aligned}$$

where $i \in [1, N]$.

3.5 Feature selection

After iterating the above steps, i.e., similarity calculation, find the nearest neighbor samples and update weight vector, T times, we jump out of the algorithm's loop. Then we get a final weight vector WT . And the average weight vector is,

$$\overline{WT} = \frac{1}{T} WT. \tag{26}$$

Then, we make feature selection based on the final \overline{WT} and threshold τ . Here, τ can be chosen to retain relevant features and discard irrelevant features [38], that is to say, those features whose weight greater than τ will be selected, and those less than τ will be discarded. Here, the value of τ is determined with regards to the user's requirements and the characteristics of the problem itself (e.g., the distribution of samples, the number of features).

4 Example

Suppose there are four samples(see Table 1), $S_0 = (1, 0, 0, 1, 0, 0)$, $S_1 = (1, 0, 0, 0, 1, 0)$, $S_2 = (0, 1, 0, 0, 0, 1)$, $S_3 = (0, 1, 0, 1, 0, 0)$, $S_4 = (0, 0, 1, 0, 1, 0)$, $S_5 = (0, 0, 1, 0, 0, 1)$, thus the n is 3, and they belong to two classes: $A = \{S_0, S_1\}$, $B = \{S_2, S_3\}$, $C = \{S_4, S_5\}$, which is illustrated in Fig. 7.

Table 1: The feature values of four samples. Each row represents all the feature values of a certain sample, while each column denotes a certain feature value of all the samples

| | F_0 | F_1 | F_2 | F_3 | F_4 | F_5 |
|-------|-------|-------|-------|-------|-------|-------|
| S_0 | 1 | 0 | 1 | 0 | 0 | 0 |
| S_1 | 1 | 0 | 0 | 0 | 1 | 0 |
| S_2 | 0 | 1 | 0 | 0 | 0 | 1 |
| S_3 | 0 | 1 | 0 | 1 | 0 | 0 |
| S_4 | 0 | 0 | 1 | 0 | 1 | 0 |
| S_5 | 0 | 0 | 1 | 0 | 0 | 1 |

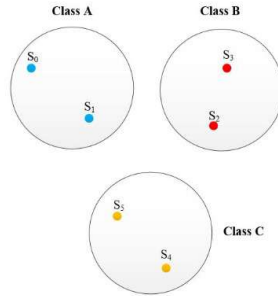


Fig. 7: The simple example with six samples in classes A , B and C .

First, the four initial quantum states are prepared as follows,

$$\begin{cases} |\psi\rangle_{S_0} = |000\rangle |0\rangle^{\otimes 3} |1\rangle |0\rangle \\ |\psi\rangle_{S_1} = |001\rangle |0\rangle^{\otimes 3} |1\rangle |0\rangle \\ |\psi\rangle_{S_2} = |010\rangle |0\rangle^{\otimes 3} |1\rangle |0\rangle \\ |\psi\rangle_{S_3} = |011\rangle |0\rangle^{\otimes 3} |1\rangle |0\rangle \\ |\psi\rangle_{S_4} = |100\rangle |0\rangle^{\otimes 3} |1\rangle |0\rangle \\ |\psi\rangle_{S_5} = |100\rangle |0\rangle^{\otimes 3} |1\rangle |0\rangle \end{cases}. \quad (27)$$

Next, we take $|\psi\rangle_{S_0}$ as an example, then the $H^{\otimes 3}$ operation is applied on the third and fourth qubits,

$$|000\rangle |0\rangle^{\otimes 3} |1\rangle |0\rangle \xrightarrow{H^{\otimes 3}} \frac{1}{2} |000\rangle \sum_{i=0}^3 |i\rangle |1\rangle |0\rangle. \quad (28)$$

Then we perform R_y rotation (see Eq. (9)) on the last qubit, and can get

$$|\phi\rangle_{S_0} = \frac{1}{2} |000\rangle \sum_{i=0}^3 |i\rangle |1\rangle \left(\sqrt{1-|\bar{v}_{0i}|^2} |0\rangle + \bar{v}_{0i} |1\rangle \right). \quad (29)$$

The other quantum states are prepared in the same way and they are listed as below,

$$\left\{ \begin{array}{l} |\phi\rangle_{S_0} = \frac{1}{2} |000\rangle \sum_{i=0}^3 |i\rangle |1\rangle \left(\sqrt{1-|\bar{v}_{0i}|^2} |0\rangle + \bar{v}_{0i} |1\rangle \right) \\ |\phi\rangle_{S_1} = \frac{1}{2} |001\rangle \sum_{i=0}^3 |i\rangle |1\rangle \left(\sqrt{1-|\bar{v}_{1i}|^2} |0\rangle + \bar{v}_{1i} |1\rangle \right) \\ |\phi\rangle_{S_2} = \frac{1}{2} |010\rangle \sum_{i=0}^3 |i\rangle |1\rangle \left(\sqrt{1-|\bar{v}_{2i}|^2} |0\rangle + \bar{v}_{2i} |1\rangle \right) \\ |\phi\rangle_{S_3} = \frac{1}{2} |011\rangle \sum_{i=0}^3 |i\rangle |1\rangle \left(\sqrt{1-|\bar{v}_{3i}|^2} |0\rangle + \bar{v}_{3i} |1\rangle \right) \\ |\phi\rangle_{S_4} = \frac{1}{2} |100\rangle \sum_{i=0}^3 |i\rangle |1\rangle \left(\sqrt{1-|\bar{v}_{4i}|^2} |0\rangle + \bar{v}_{4i} |1\rangle \right) \\ |\phi\rangle_{S_5} = \frac{1}{2} |101\rangle \sum_{i=0}^3 |i\rangle |1\rangle \left(\sqrt{1-|\bar{v}_{5i}|^2} |0\rangle + \bar{v}_{5i} |1\rangle \right) \end{array} \right. \quad (30)$$

Second, we randomly select a sample (assume $|\phi\rangle_{S_0}$ is \bar{u}), and perform similarity calculation with other samples (i.e., $|\phi\rangle_{S_1}, |\phi\rangle_{S_2}, |\phi\rangle_{S_3}, |\phi\rangle_{S_4}, |\phi\rangle_{S_5}$). Next, we take $|\phi\rangle_{S_0}$ and $|\phi\rangle_{S_1}$ as an example, and perform a *swap* operation between the last two qubits of $|\phi\rangle_{S_0}$,

$$|\phi\rangle_{S_0} \xrightarrow{swap} |\varphi\rangle = \frac{1}{2} |000\rangle \sum_{i=0}^3 |i\rangle \left(\sqrt{1-|\bar{v}_{0i}|^2} |0\rangle + \bar{v}_{0i} |1\rangle \right) |1\rangle. \quad (31)$$

After that, the *swap test* operation is applied on $(|\varphi\rangle, |\phi\rangle_{S_1})$,

$$\frac{1}{2} |0\rangle (|\varphi\rangle |\phi\rangle_{S_1} + |\phi\rangle_{S_1} |\varphi\rangle) + \frac{1}{2} |1\rangle (|\varphi\rangle |\phi\rangle_{S_1} - |\phi\rangle_{S_1} |\varphi\rangle). \quad (32)$$

We perform a *swap test* operation to obtain a quantum state that encodes similarity in amplitude

$$\left\{ \begin{array}{l} |\alpha\rangle_A = \frac{1}{\sqrt{2}} \sum_{q=1}^2 |q\rangle \left(\sqrt{1-s(\bar{u}, \bar{v}_q)} |0\rangle + \sqrt{s(\bar{u}, \bar{v}_q)} |1\rangle \right) \\ |\alpha\rangle_B = \frac{1}{\sqrt{2}} \sum_{q=1}^2 |q\rangle \left(\sqrt{1-s(\bar{u}, \bar{v}_q)} |0\rangle + \sqrt{s(\bar{u}, \bar{v}_q)} |1\rangle \right) \\ |\alpha\rangle_C = \frac{1}{\sqrt{2}} \sum_{q=1}^2 |q\rangle \left(\sqrt{1-s(\bar{u}, \bar{v}_q)} |0\rangle + \sqrt{s(\bar{u}, \bar{v}_q)} |1\rangle \right) \end{array} \right. \quad (33)$$

Then through the amplitude estimation, we can obtain the quantum states,

$$\begin{cases} |\beta\rangle_A = \frac{1}{\sqrt{2}} \sum_{q=1}^2 |q\rangle |\bar{v}_q - \bar{u}\rangle \\ |\beta\rangle_B = \frac{1}{\sqrt{2}} \sum_{q=1}^2 |q\rangle |\bar{v}_q - \bar{u}\rangle. \\ |\beta\rangle_C = \frac{1}{\sqrt{2}} \sum_{q=1}^2 |q\rangle |\bar{v}_q - \bar{u}\rangle \end{cases} \quad (34)$$

Next, we perform an oracle operation on the quantum states obtained in the above steps to obtain the k nearest neighbor samples.

5 Simulation Experiment

Quantum Cloud Services (QCS^{TM}) is Rigetti’s quantum-first cloud computing platform. At the end of 2017, a 19-qubit processor named ‘Acorn’ was launched, which can be used in QCS through a quantum programming toolkit named Forest [39]. The chip of ‘Acorn’ is made of 20 superconducting qubits but for some technical reasons, qubit 3 is off-line and cannot interact with its neighbors, so it is treated as a 19-qubit device whose coupling map is shown in Fig. 8.

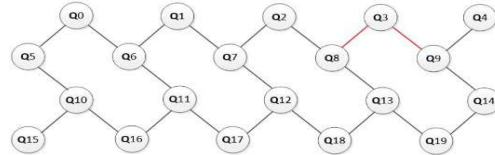


Fig. 8: The coupling map picture: Rigetti’s 19-qubit processor ‘Acorn’. Lines indicate the two-qubit connection ruled by a controlled-Z operation.

In order to obtain the result and also verify our algorithm, we choose Rigetti to perform the quantum processing. However, since the Rigetti platform limits the length of the entire circuit and noise has a great influence on the preparation of quantum states [40], we only show one of the ideal experiment circuits of similarity calculation in QRelief algorithm running on Rigetti platform. We successfully stored the characteristic information in the sample into the amplitude of the quantum state, and then extracted the amplitude information into the quantum state through the phase estimation algorithm. Fig. 9 gives the schematic diagram of our experimental circuit. The corresponding code of the circuit in Rigetti is shown in Program 3. After running 8 times of Program 3, the result can be seen in Fig. 10. We can get $|1\rangle$ with the average probability of 0.435125. Then we successfully stored the characteristic information in the sample into the amplitude of the quantum state. According to Eq. (33), we can

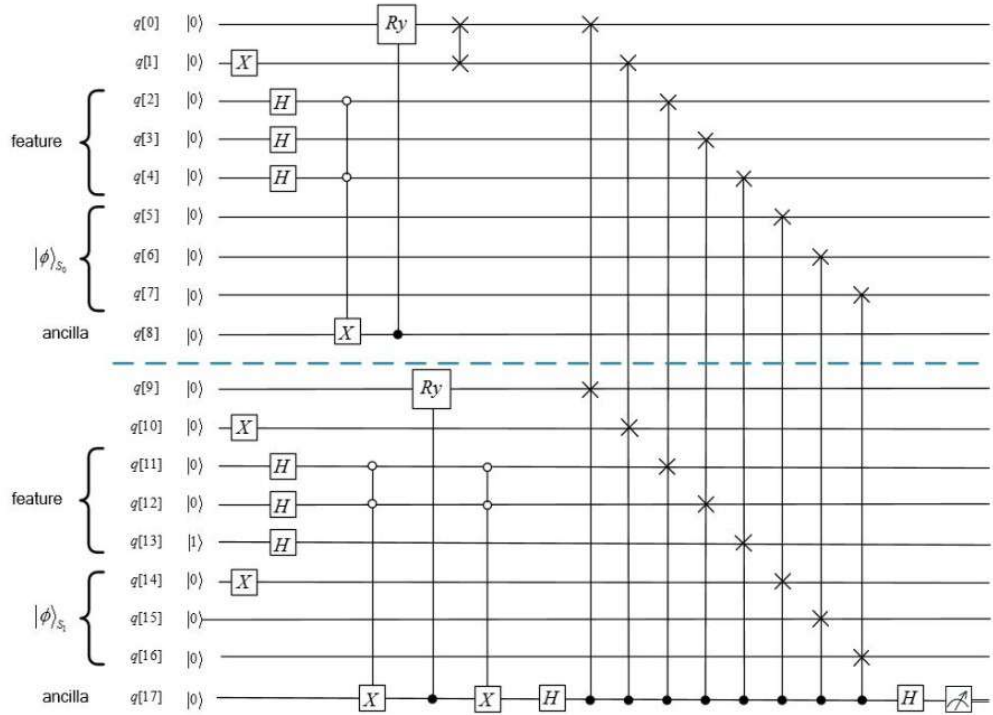


Fig. 9: One of the ideal experiment circuits of similarity calculation in QReliefF algorithm running on Rigetti platform. $q[0] - q[7]$ represents the randomly selected quantum state $|\phi\rangle_{S_0}$, $q[9] - q[16]$ represents $|\phi\rangle_{S_1}$, and $q[17]$ is the result qubit. X is the Not operation, and Ry is R_y operation which can be expressed as a matrix in Eq. (9).

get $\sqrt{s(\bar{u}, \bar{v}_q)} \approx \sqrt{0.435}$, i.e., $s(\bar{u}, \bar{v}_q) \approx 0.435$, and then extracted the amplitude information into the quantum state through the phase estimation algorithm.

Program 3: Similarity calculation in QRelief algorithm running on Rigetti

```

1  # Define the new gate from a matrix
2  theta = Parameter('theta')
3  cry = np.array([
4      [1, 0, 0, 0],
5      [0, 1, 0, 0],
6      [0, 0, quil_sqrt(1 - theta * theta), -theta * theta],
7      [0, 0, theta * theta, quil_sqrt(1 - theta * theta)]
8  ]);
9  gate_definition = DefGate('CRY', cry, [theta])
10 CRY = gate_definition.get_constructor()
11 # Create our program and use the new parametric gate
12 p = Program(
13     gate_definition, X(1), H(2), H(4), H(5), X(2), X(5),
14     CCNOT(2, 5, 18), X(2), X(5), CRY(1)(18, 0),
15     SWAP(0, 1), X(10), H(11), H(12), H(13), X(14),
16     X(11), X(12), CCNOT(11, 12, 17), X(11), X(12),
17     CRY(1)(17, 9), H(19), CSWAP(19, 0, 9),
18     CSWAP(19, 1, 10), CSWAP(19, 2, 11),
19     CSWAP(19, 4, 12), CSWAP(19, 5, 13),
20     CSWAP(19, 6, 14), CSWAP(19, 7, 15),
21     CSWAP(19, 8, 16), H(19)
22 )
23 #print the circuit
24 print(p)
25 # get a QPU, 20q-Acorn is just a string naming the device
26 qc = get_qc('20q - Acorn')
27 # run and measure
28 result = qc.run_and_measure(p, trials = 1024)

```

After all the steps have been performed, we obtain the quantum states S_1 (H), S_2 ($M(B)$) and S_5 ($M(C)$) of the nearest neighbor samples of the quantum state S_0 (\bar{u}) in each class of the random sample which can be seen in Fig. 11. Then, the weight vectors are updated according to Eq. (25) and the result of WT is listed in the second row of Table 2 after the first iteration. The algorithm iterates T times (in our example, $T=4$) as above steps, and obtains all the WT results shown in Table 2. After T -th iterations, $WT = [4, 4, 4, -2, 0, -2]$, then $\overline{WT} = [1, 1, 1, -1/2, 0, -1/2]$. In this paper, the value of τ in the example is assumed to be 0.5 according to the updated result of WT in TABLE 2. Since the threshold $\tau = 0.5$, so the selected features are F_0 , F_1 and F_2 , i.e., the first,

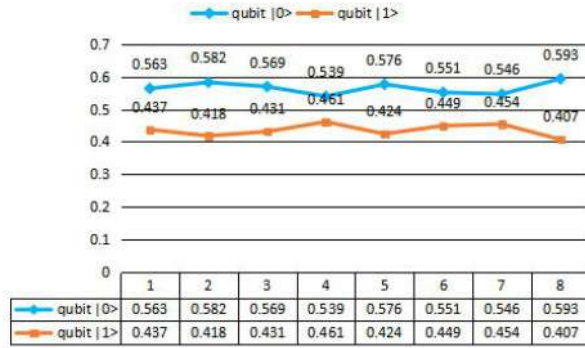


Fig. 10: The measurement result of $|0\rangle$ and $|1\rangle$ after running 8 times of Program 3 on Rigetti.

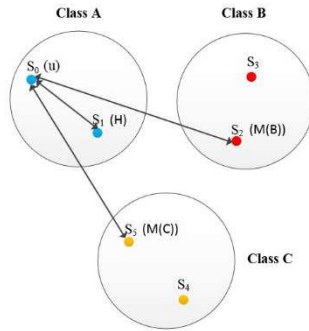


Fig. 11: Finding the nearest neighbor samples (S_1 , S_2 and S_3) of the sample S_0 .

Table 2: The updated result of WT

| $Iteration\ times(T)$ | $Weight\ vector(WT)$ |
|-----------------------|----------------------|
| 1 | [1 1 1 0 0 -1] |
| 2 | [2 2 2 -1 0 -1] |
| 3 | [3 3 3 -1 0 -2] |
| 4 | [4 4 4 -2 0 -2] |

second and third features. The result of quantum feature selection is consistent with the classical ReliefF algorithm after being verified by python.

In the final weight value comparison, considering the large amount of data in the complex system and the corresponding eigenvalues, the calculation amount required for the comparison after the final result is obtained is also large. In order to meet the requirements of big data and result accuracy, we adopted an optimized quantum maximum and minimum value search algorithm [37] when comparing weights in the last step to help us quickly and accurately select the features we want, so as to better solve the multi-classification problem in complex systems.

In circumstances when we can exactly estimate the ratio of the number of solutions M and the searched space N , this algorithm can improve the successful probability close to 100%. Furthermore, it shows an advantage in complexity with large databases and in the operation complexity of constructing oracles.

6 Efficiency analysis

In order to evaluate the efficiency of QReliefF algorithm, three algorithms (i.e., classical Relief, classical ReliefF, quantum Relief algorithms) are selected to compare with our algorithm from three indicators: complexity of similarity calculation (CSC), complexity of finding the nearest neighbor (CFNN) and resource consumption (RC).

In the classic Relief algorithm, it takes $O(N)$ time to calculate the distance between randomly selected samples and any other samples, and then finds the nearest neighbors related to M . This process needs to iterate T times, so CSC is $O(TMN)$. Since T is a constant, then CSC in the classic Relief algorithm is $O(MN)$. As we know, there are totally M samples, each with N features, so CFNN is $O(M)$ and RC in the classic Relief algorithm is $O(MN)$ bits. The classical ReliefF algorithm is similar to the classical Relief algorithm. Since it finds k nearest neighbors at once time, so the time complexity is $O(kTMN)$. Then we can simplify CSC to $O(MN)$ because k and T are constants. Besides, CFNN for finding k nearest neighbors is $O(M)$. In terms of resource consumption, there are M samples, each sample has N features, so the resource consumption of the classic ReliefF algorithm is $O(MN)$ bits.

In QRelief and QReliefF algorithms, the quantum property is used to calculate the distance from $O(N)$ to $O(1)$, so their CSCs are all $O(TM)$. Since T is constant, their CSCs can be simplified to $O(M)$. CFNN of QRelief is $O(kM)$, then it can be simplified to $O(M)$ as k is constant. While CFNN of QReliefF is \sqrt{kM} because it uses the quantum Grover-Long method to find k nearest neighbor samples which holds a quadratic acceleration. Since k is constant, CFNN of QReliefF is $O(\sqrt{M})$. RC of similarity calculation, finding the nearest neighbor samples and updating weight vector are $O(TM \log N)$, $O(TN)$ and $O(N)$, respectively. Therefore, the total complexity is $O(TM \log N + TN + N)$, since T is constant, then RC of QRelief and QReliefF are all $O(M \log N + N)$. For multi-features big data in complex systems with edge computing, there is

$M \gg N$, so $M \gg \frac{N}{N - \log N}$, then RC of QRelief and QReliefF can be simplified into $O(M \log N)$.

For convenience, we list the efficiency comparison of classic Relief algorithm, ReliefF algorithm, quantum Relief algorithm and our algorithm in terms of CSC, CFNN and RC in Table 3. Obviously, our algorithm is superior than classical algorithms (i.e., Relief and ReliefF) in terms of CSC, CFNN and RC, and better than quantum algorithm (i.e., QRelief) in terms of CFNN.

Table 3: Efficiency comparison between classical Relief, classical ReliefF, QRelief and our QReliefF algorithms

| | Multi-classification | CSC | CFNN | RC |
|----------|----------------------|---------|---------------|---------------|
| Relief | no | $O(MN)$ | $O(M)$ | $O(MN)$ |
| ReliefF | yes | $O(MN)$ | $O(M)$ | $O(MN)$ |
| QRelief | no | $O(M)$ | $O(M)$ | $O(M \log N)$ |
| QReliefF | yes | $O(M)$ | $O(\sqrt{M})$ | $O(M \log N)$ |

7 Conclusion and discussion

With the rapid development of edge computing technology and quantum machine learning algorithms, researchers began to pay attention to the combination and application of these two fields. In this paper, we use quantum technology to solve the multi-classification problem of feature selection in the complex systems with edge computing, and propose a quantum ReliefF algorithm. Compared to the classic ReliefF algorithm, our algorithm reduces the complexity of similarity calculation from $O(MN)$ to $O(M)$, and the complexity of finding the nearest neighbor from $O(M)$ to $O(\sqrt{M})$. In addition, from the perspective of resource consumption, our algorithm consumes $O(M \log N)$ qubit, while the classic ReliefF algorithm consumes $O(MN)$ bit. Obviously, our algorithm is superior in terms of computational complexity and resource consumption.

It should be noted that our work aims to improve the algorithm efficiency, while the privacy protection of sensitive data is not taken into account. At present, data security has become a focus of attention in the field of artificial intelligence, some solutions for data privacy protection in complex systems with edge computing have been proposed [41] [42] [43] [44]. In our future work, how to improve the efficiency of quantum machine learning algorithms while ensuring the privacy protection of sensitive data, such as [45] [46] [47] [48], will become our direction.

Acknowledgment

The authors would like to express heartfelt gratitude to the anonymous reviewers and editor for their comments that improved the quality of this paper. And the

support of all the members of the quantum research group of NUIST & SEU is especially acknowledged, their professional discussions and advices have helped us a lot.

References

1. Roberta Alfieri and Luciano Milanese, “Complex System,” Springer New York, New York, 2013.
2. Michael Armbrust, Armando Fox, Rean Griffith, Anthony D. Joseph, Randy Katz, Andy Konwinski, Gunho Lee, David A. Patterson, Ariel Rabkin, Ion Stoica and Matei Zaharia, “A View of Cloud Computing,” *Communications of the ACM*, vol. 53, no. 4, pp. 50-58, 2010.
3. Xu Chen, Lei Jiao, Wenzhong Li and Xiaoming Fu, “Efficient Multi-User Computation Offloading for Mobile-Edge Cloud Computing,” *IEEE/ACM Transactions on Networking*, vol. 24, no. 5, pp. 2827-2840, 2016.
4. Xiaolong Xu, Shucun Fu, Lianyong Qi, Xuyun Zhang, Qingxiang Liu, Qiang He and Shang Li, “An IoT-Oriented Data Placement Method with Privacy Preservation in Cloud Environment,” *Journal of Network and Computer Applications*, vol. 124, pp. 148-157, 2018.
5. Lianyong Qi, Yi Chen, Yuan Yuan, Shucun Fu, Xuyun Zhang and Xiaolong Xu, “A QoS-Aware Virtual Machine Scheduling Method for Energy Conservation in Cloud-based Cyber-Physical Systems,” *World Wide Web*, 2019. DOI:10.1007/s11280-019-00684-y.
6. Yuyi Mao, Changsheng You, Jun Zhang, Kaibin Huang and Khaled B. Letaief, “A Survey on Mobile Edge Computing: The Communication Perspective,” *IEEE Communications Surveys and Tutorials*, vol. 19, no. 4, pp. 2322-2358, 2017.
7. Xiaolong Xu, Yuancheng Li, Tao Huang, Yuan Xue, Kai Peng, Lianyong Qi and Wanchun Dou, “An Energy-Aware Computation Offloading Method for Smart Edge Computing in Wireless Metropolitan Area Networks,” *Journal of Network and Computer Applications*, vol. 133, pp. 75-85, 2019.
8. Lianyong Qi, Xuyun Zhang, Wanchun Dou, Chunhua Hu, Chi Yang and Jinjun Chen, “A Two-stage Locality-Sensitive Hashing Based Approach for Privacy-Preserving Mobile Service Recommendation in Cross-Platform Edge Environment,” *Future Generation Computer Systems*, vol. 88, pp. 636-643, 2018.
9. Xiaolong Xu, Xuyun Zhang, Honghao Gao, Yuan Xue, Lianyong Qi and Wanchun Dou, “BeCome: Blockchain-Enabled Computation Offloading for IoT in Mobile Edge Computing,” *IEEE Transactions on Industrial Informatics*, 2019. DOI:10.1109/TII.2019.2936869.
10. Mehryar Mohri, Afshin Rostamizadeh and Ameet Talwalkar, “Foundations of Machine Learning,” MIT Press, 2012.
11. Xiaolong Xu, Yi Chen, Xuyun Zhang, Qingxiang Liu, Xihua Liu and Lianyong Qi, “A Blockchain-based Computation Offloading Method for Edge Computing in 5G Networks,” *Software: Practice and Experience*, 2019. DOI:10.1002/spe.2749.
12. Gunasekaran Manogaran, Daphne Lopez and Naveen Chilamkurti, “In-Mapper Combiner based MapReduce Algorithm for Processing of Big Climate Data,” *Future Generation Computer Systems*, vol. 86, pp. 433-445, 2018.
13. Lianyong Qi, Ruili Wang, Shancang Li, Qiang He, Xiaolong Xu and Chunhua Hu, “Time-aware Distributed Service Recommendation with Privacy-preservation,” *Information Sciences*, vol. 480, pp. 354-364, 2019.

14. Xiaolong Xu, Qingxiang Liu, Yun Luo, Kai Peng, Xuyun Zhang, Shunmei Meng, and Lianyong Qi, "A Computation Offloading Method over Big Data for IoT-enabled Cloud-edge Computing," *Future Generation Computer Systems*, vol. 95, pp. 522-533, 2019.
15. Ronald A. Howard, "Dynamic Programming," *Management Science*, vol. 12, no. 5, pp. 317-348, 1966.
16. Sam T. Roweis and Lawrence K. Saul, "Nonlinear dimensionality reduction by locally linear embedding," *Science*, vol. 290, no. 5500, pp. 2323-2326, 2005.
17. Huan Liu, "Feature Selection for Knowledge Discovery and Data Mining," Springer, New York, 2012.
18. Kenji Kira and Larry A. Rendell, "A Practical Approach to Feature Selection," *Proceedings of the Ninth International Workshop on Machine Learning*, Aberdeen, Scotland, UK, 1992.
19. Igor Kononenko, "Estimating Attributes: Analysis and Extensions of Relief," In: *Machine Learning: ECML-94*. Springer, Berlin, Heidelberg, vol. 784, 2005.
20. Yi Zhang, Chris Ding, and Tao Li, "Gene Selection Algorithm by Combining Relief and MRMR," *BMC Genomics*, vol. 9, no. 2, pp. S27, 2008.
21. Deguang Kong, Carolina Ding, Heng Huang and Haifeng Zhao, "Multi-label Relief and F-statistic Feature Selections for Image Annotation." *IEEE Conference on Computer Vision and Pattern Recognition*, vol. 1, pp. 2352-2359, 2012.
22. Jason H. Moore, "Epistasis Analysis Using ReliefF," *Epistasis: Methods and Protocols*, Springer New York, pp. 315-325, 2015.
23. Paul Benioff, "The Computer as a Physical System: A Microscopic Quantum Mechanical Hamiltonian Model of Computers as Represented by Turing Machines," *Journal of Statistical Physics*, vol. 22, no. 5, pp. 563-591, 1980.
24. Richard P. Feynman, "Simulating Physics with Computers," *International Journal of Theoretical Physics*, vol. 21, no. 6-7, pp. 467-488, 1982.
25. Peter W. Shor, "Polynomial-Time Algorithms for Prime Factorization and Discrete Logarithms on a Quantum Computer," *SIAM Review*, vol. 41, no. 2, pp. 303-332, 1999.
26. Lov K. Grover, "Quantum Mechanics Helps in Searching for a Needle in a Haystack," *Physical Review Letters*, vol. 79, no. 2, pp. 325-328, 1997.
27. Zhiguo Qu, Tiancheng Zhu, Jinwei Wang and Xiaojun Wang, "A Novel Quantum Steganography Based on Brown States," *Cmc-Computers, Materials & Continua*, vol. 56, no. 1, pp. 47-59, 2018.
28. Wenjie Liu, Peipei Gao, Yuxiang Wang, Wenbin Yu and Maojun Zhang, "A Unitary Weights Based One-Iteration Quantum Perceptron Algorithm for Non-Ideal Training Sets," *IEEE Access*, vol. 7, pp. 36854-36865, 2019.
29. Wenjie Liu, Peipei Gao, Zhihao Liu, Hanwu Chen and Maojun Zhang, "A Quantum-Based Database Query Scheme for Privacy Preservation in Cloud Environment," *Security and Communication Networks*, vol. 2019, pp. 14, 2019.
30. Lucas Lamata, Mikel Sanz and Enrique Solano, "Quantum Machine Learning and Bioinspired Quantum Technologies," *Advanced Quantum Technologies*, vol. 2, pp. 7-8, 2019.
31. Zhiguo Qu, Zhengyan Li, Gang Xu, Shengyao Wu and Xiaojun Wang, "Quantum Image Steganography Protocol Based on Quantum Image Expansion and Grover Search Algorithm," *IEEE Access*, vol. 7, pp. 50849-50857, 2019.
32. Zhiguo Qu, Zhenwen Cheng and Xiaojun Wang, "Matrix Coding-Based Quantum Image Steganography Algorithm," *IEEE Access*, vol. 7, pp. 35684-35698, 2019.
33. Wenjie Liu, Peipei Gao, Wenbin Yu, Zhiguo Qu and Chingnung Yang, "Quantum Relief Algorithm," *Quantum Information Processing*, vol. 17, no. 10, pp. 280, 2018.

34. Michael A. Nielsen and Isaac L. Chuang, "Quantum Computation and Quantum Information," Cambridge University press, United Kingdom, pp. 221, 2000.
35. Guilu Long, "Grover Algorithm with Zero Theoretical Failure Rate," *Physical Review A*, vol. 64, no. 2, pp. 022307, 2001.
36. SiSi Zhou, Thomas Loke, J A Izaac, Jingbo Wang, "Quantum Fourier transform in computational basis," *Quantum Information Processing*, vol. 16, no. 3, 2017.
37. Yanhu Chen, Shijie Wei, Xiong Gao, Cen Wang, Jian Wu and Hongxiang Guo, "An Optimized Quantum Maximum or Minimum Searching Algorithm and its Circuits," arXiv:1908.07943, 2019.
38. Kenji Kira and Larry A. Rendell, "Feature selection problem: traditional methods and a new algorithm," *Proceedings Tenth National Conference on Artificial Intelligence*, pp. 129-134, 1992.
39. Robert S. Smith, Michael J. Curtis and William J. Zeng, "A Practical Quantum Instruction Set Architecture," arXiv:1608.03355v2, 2017.
40. Zhiguo Qu, Shengyao Wu, Mingming Wang, Le Sun and Xiaojun Wang, "Effect of Quantum Noise on Deterministic Remote State Preparation of an Arbitrary Two-Particle State via Various Quantum Entangled Channels," *Quantum Information Processing*, vol. 16, no. 306, pp. 1-25, 2017.
41. Xiaolong Xu, Chengxun He, Zhanyang Xu, Lianyong Qi, Shaohua Wan and MZA Bhuiyan, "Joint Optimization of Offloading Utility and Privacy for Edge Computing Enabled IoT," *IEEE Internet of Things Journal*, 2019. DOI:10.1109/JIOT.2019.2944007.
42. Hu Xiong, Yanan Zhao, Li Peng, Hao Zhang and Kuohui Yeh, "Partially Policy-hidden Attribute-based Broadcast Encryption with Secure Delegation in Edge Computing," *Future Generation Computer Systems-The International Journal of Escience*, vol. 97, pp. 453-461, 2019.
43. Jiale Zhang, Bing Chen, Yanchao Zhao, Xiang Cheng and Feng Hu, "Data Security and Privacy-Preserving in Edge Computing Paradigm: Survey and Open Issues," *IEEE Access*, vol. 6, pp. 18209-18237, 2018.
44. Xiaolong Xu, Yuan Xue, Lianyong Qi, Yuan Yuan, Xuyun Zhang, Tariq Umer and Shaohua Wan, "An Edge Computing-enabled Computation Offloading Method with Privacy Preservation for Internet of Connected Vehicles," *Future Generation Computer Systems*, vol. 96, pp. 89-100, 2019.
45. Wenjie Liu, Zhenyu Chen, Jinsuo Liu, Zhaofeng Su and Lianhua Chi, "Full-Blind Delegating Private Quantum Computation," *Cmc-Computers Materials & Continua*, vol. 56, no. 2, pp. 211-223, 2018.
46. Wenjie Liu, Yong Xu, Haibin Wang and Zhibin Lei, "Quantum Searchable Encryption for Cloud Data Based on Full-Blind Quantum Computation," *IEEE Access*, vol. 7, pp. 186284-186295, 2019.
47. Wenjie Liu, Yong Xu, James C. N. Yang, Wenbin Yu and Lianhua Chi, "Privacy-Preserving Quantum Two-Party Geometric Intersection," *Cmc-Computers, Materials & Continua*, vol. 60, no. 3, pp. 1237-1250, 2019.
48. Wenjie Liu, Yinsong Xu, Maojun Zhang, Junxiu Chen and Chingnung Yang, "A Novel Quantum Visual Secret Sharing Scheme," *IEEE Access*, vol. 7, pp. 114374-114384, 2019.